Hindawi Publishing Corporation
International Journal of Rotating Machinery
Volume 2008, Article ID 387828, 12 pages
doi:10.1155/2008/387828

Research Article

Reduced-Order Model Development for Airfoil Forced Response

Jeffrey M. Brown[1] and Ramana V. Grandhi[2]

[1] *Turbine Engine Division, US Air Force Research Lab/RZTS, 1950 5th Street, Building 18, Wright-Patterson AFB, OH 45433, USA*
[2] *Department of Mechanical and Materials Engineering, Wright State University, 3640 Colonel Gelnn Hwy, Dayton, OH 45435, USA*

Correspondence should be addressed to Jeffrey M. Brown, jeffrey.brown@wpafb.af.mil

Received 9 July 2007; Accepted 2 January 2008

Recommended by Toshinori Watanabe

Two new reduced-order models are developed to accurately and rapidly predict geometry deviation effects on airfoil forced response. Both models have significant application to improved mistuning analysis. The first developed model integrates a principal component analysis approach to reduce the number of defining geometric parameters, semianalytic eigensensitivity analysis, and first-order Taylor series approximation to allow rapid as-measured airfoil response analysis. A second developed model extends this approach and quantifies both random and bias errors between the reduced and full models. Adjusting for the bias significantly improves reduced-order model accuracy. The error model is developed from a regression analysis of the relationship between airfoil geometry parameters and reduced-order model error, leading to physics-based error quantification. Both models are demonstrated on an advanced fan airfoil's frequency, modal force, and forced response.

1. INTRODUCTION

Effective airfoil dynamic response analysis ensures rotor reliability and requires prediction of resonance avoidance margin, forced response, and mistuning. Standard practices predict dynamic response using finite element models (FEMs) of design intent geometries. While sufficient for some cases, this standard approach does not explicitly consider airfoil structural response variations caused by random manufacturing deviations from design intent geometries. Because hundreds or thousands of these simulations would be required to assess effects from random variations, a new more efficient airfoil modal and a forced response prediction process are required.

Existing literature contains a significant body of work developing efficient mistuned rotor forced response prediction using reduced-order models (ROMs) [1–6]. These efforts have shown strong amplification of rotor forced response caused by small perturbations in blade-to-blade frequency. While effective, these prior models are limited in two significant ways. First, they assume that airfoil frequencies vary, but airfoil mode shapes remain nominal. This assumption enables computational efficiencies but geometric deviations clearly alter blade-to-blade mode shapes, thus altering each blade's modal force and impacting mistuned response. Their second limitation is the required experimentally obtained blade-to-blade frequency variation input. Such empirical measures are subject to error, particularly for integrally bladed rotors (IBRs) and the known challenge to isolate their individual airfoil frequencies from the rotor system response. These experimental results also are not connected to airfoil geometric parameters that can be controlled in the design process for acceptable frequency scatter manufacturing. Because of these limitations, physics-based ROMs of airfoil modal and forced response that explicitly account for geometric deviations are needed as they provide accurate input to existing mistuning models and include frequency scatter in design. Further, since existing mistuning prediction methods do not consider mode shape variation, a ROM is needed to show the significance of mode shape variation on forced response and leads to future improved mistuning analysis tools.

ROM development begins with an approach to create a reduced set of geometry parameters defining manufacturing variation. Previous efforts in reduced-order airfoil geometry modeling include Garzon and Darmofal's use of principal

component analysis (PCA) [7]. The PCA approach is a common statistical method that creates a reduced basis space through an eigenanalysis of the covariance between parameter deviations [8]. The research's results demonstrate the effectiveness of the technique for turbomachinery applications. An alternate approach was demonstrated by Capiez-Lernout et al. in their development of a technique characterizing manufacturing tolerances for mistuned bladed disk with a dispersion parameter [9]. This ad-hoc estimation of the geometry effects on response does not directly depend on measured geometry but does have computational advantages. Because the PCA approach is directly related to measured deviations, it is applied in this ROM development.

With a reduced geometry model determined, development of a reduced-order response method remains. Taylor series approximations are an attractive method assuming that the required sensitivities can be efficiently calculated. Methods to rapidly predict sensitivities of modal response, eigensensitivities, have been developed by Fox and Kapoor for unique eigenproblems and Friswell for cyclic symmetry problems [10, 11]. These equations are semianalytic and allow sensitivity calculation from a single FEM solution with efficiency improvements described later. Such approaches have been widely used in optimization applications, but not for airfoil modal response approximation over the range of manufacturing deviations considered in this effort.

With these existing tools, the first of two airfoil response ROMs, the standard ROM, is developed. First, PCA is used to create a reduced basis set of the manufacturing deviations. Eigensensitivities are then efficiently calculated semianalytically with respect to this new basis, and these are used in a first-order Taylor series modal response approximation. These approximate modal quantities are then used in a modal domain forced response analysis. When combined, the integrated approaches lead to an exceptionally efficient and accurate model.

Though accurate, as with all approximations, there is error. Model errors have been widely recognized as critical to the design and analysis process, and the need for their accounting has been outlined in several professional editorial policy papers [12, 13]. In this research, a second ROM is developed, an error-quantified ROM, that captures the error developed in the model reduction process. This a posterior error model requires a linear regression model of the errors obtained between a limited number of full model and standard ROM comparisons. Results from the model are able to reduce the standard ROM error and quantify the approximate model uncertainty.

It is noted that these models do not account for the impact of geometric deviations on unsteady aerodynamic loading. While this may be an important factor in the prediction of forced response, the development of a reduced-order model for aerodynamics is an ongoing challenge not considered in this research.

The following sections develop the two ROMs. How measured airfoil deviations are reduced to a practical number of parameters with PCA is defined in Section 2. Section 3 develops the standard reduced-order modal and forced response models, and Section 4 introduces the error-quantified ROM. These sections are followed by results from a real-world component that show the significance of geometric deviations from design intent and demonstrate the accuracy of both developed models. The application of these new tools provides improved input to existing mistuning prediction models that show the effect of geometrically induced mode shape variation on forced response and create a model that can be used for future mistuning tool developments.

2. REDUCED-ORDER AIRFOIL GEOMETRY MODEL

In the past, deviations from design intent have been checked with shaped tools and manual gages. Such devices are pass-fail tools providing no quantitative response information back to the engineer. Because of the rotor response sensitivity to geometric variations, new measurement techniques are desired. One approach uses coordinate measurement machines (CMMs) that collect data through a geometry traversing probe that obtains spatial data points at regular intervals. Each measured airfoil may provide thousands of measured data points. Assessing the sensitivity of each of these locations to perturbation would require significant computational resources, hence the need for a reduced-order geometry model retaining a limited set of parameters quantifying geometry deviations. PCA is attractive given its ease of implementation and the creation of minimum, a set of retained basis vectors to represent correlated geometry variations.

PCA is implemented by storing n measured three-dimensional coordinate data points in vector $\mathbf{x} \in \mathbb{R}^{3n}$. A set of p measured airfoils results in matrix, $\mathbf{X} \in \mathbb{R}^{3n,p}$. Since we are interested in variations from the average blade, the mean value of each row is subtracted from each member of the row to give a matrix of measured deviations, $\Delta\mathbf{X}$, where each element is

$$\Delta x_{i,j} = x_{i,j} - \overline{x}_i, \quad i = 1, 2, \ldots, 3n; \; j = 1, 2, \ldots, p, \tag{1}$$

where $\overline{x}_i$ is the average of the ith row. It is important to note that the average, $\overline{x}_i$, is not necessarily the original design intent. Also, subtracting the row mean from each element makes the expected value of each row zero. The first-order covariance matrix of $\Delta\mathbf{X}$ defines the statistical relationship between a measurement point deviation and all other points, and its eigensolution leads to eigenvectors that can be used to form a new subspace optimally representing variation. This is written in standard eigenproblem form:

$$\mathrm{Cov}(\Delta\mathbf{X})\boldsymbol{\Psi} = \boldsymbol{\Psi}\mathbf{D}, \tag{2}$$

where $\mathbf{D}$ and $\boldsymbol{\Psi}$ are the eigenvalue and eigenvector matrices, respectively. The eigenvectors are the principal components modes of the measured data, and the eigenvalues are the principal component variances that indicate the data variance each principal component captures. Based on these eigenvalues, graphical and statistical methods can be used to retain a limited set of basis vectors. Also of importance, the principal components are orthogonal, and therefore, uncorrelated statistically. The PCA transforms a large set

of correlated parameters into a small set of uncorrelated parameters.

Transformation of the measured deviations, $\Delta\mathbf{X}$, to the principal component basis requires the linear operation:

$$\mathbf{Z} = \mathbf{\Psi}^T[\Delta\mathbf{X}], \tag{3}$$

where the eigenfunction matrix is multiplied by the deviation matrix to give the z-score matrix, $\mathbf{Z} \in \mathbb{R}^{m,p}$ with m the number of retained principal component modes. These scores are effectively regression coefficients for the new principal component basis and define the participation of each PCA mode in each measured geometry. The above algorithms, (1)–(3), are the covariance method of PCA, and the columns of $\mathbf{Z}$ represent the Karhunen-Loeve transformation.

How these z-scores and principal component modes are integrated into a reduced-order forced response model is described in the following section.

3. STANDARD BLADE-ALONE FORCED RESPONSE REDUCED-ORDER MODEL

The approach used in this ROM development is Taylor series approximation using first-order sensitivities. Sensitivity calculations can be computationally expensive when calculated numerically via finite difference methods that require an FEM evaluations for each design parameter. This work proposes to use semianalytic methods that replace the costly calculations of the process, that is, decomposing the stiffness and mass matrix and solving the matrix eigenvalue problem.

Combining the semianalytic sensitivity methods defined in [14] with the reduced-order geometry model results from Section 2 leads to the following principal component mode response sensitivities:

$$\begin{aligned}\frac{\partial\lambda_i}{\partial\psi_j} &= \phi_i^T\left(\frac{\partial\mathbf{K}}{\partial\psi_j} - \lambda_i\frac{\partial\mathbf{M}}{\partial\psi_j}\right)\phi_i,\\ \frac{\partial\phi_i}{\partial\psi_j} &= \sum_{g=1}^{r} c_{ig}\phi_g,\end{aligned} \tag{4}$$

where i identifies the vibration mode number, j is the principal component mode number, and r is the total number of retained vibration modes. The constant terms are calculated:

$$\begin{aligned}c_{ig} &= \frac{\phi_g^T(\partial\mathbf{K}/\partial\psi_j - \lambda_g(\partial\mathbf{M}/\partial\psi_j))\phi_i}{(\lambda_g - \lambda_i)},\\ c_{ii} &= -\frac{1}{2}\phi_i^T\frac{\partial\mathbf{M}}{\partial\psi_j}\phi_i,\end{aligned} \tag{5}$$

where λ_i and ϕ_i are eigenvalue and mass-normalized eigenvector, $\mathbf{K}$ and $\mathbf{M}$ are mass and stiffness matrices, and ψ_j are retained principal component modes. The stiffness and mass matrix derivatives are numerically computed through nominal and perturbed finite element models. Forced response sensitivity can also be calculated directly but is not done so here because of the need to explicitly retain frequency and mode shape sensitivities for use as input to mistuning and modal force predictions.

Prediction of modal stress sensitivity requires the derivative of the strain-displacement equation. Differentiating this equation with respect to the jth principal component mode gives

$$\frac{\partial\sigma_i}{\partial\psi_j} = \mathbf{DB}\frac{\partial\phi_i}{\partial\psi_j} + \mathbf{D}\frac{\partial\mathbf{B}}{\partial\psi_j}\phi_i, \tag{6}$$

where $\mathbf{D}$ is the elasticity matrix, $\mathbf{B}$ is the strain-displacement matrix, and σ_i is the stress vector of the ith vibration mode. As with the mass and stiffness matrices, the sensitivity of the strain-displacement matrix is calculated numerically.

Once the sensitivities have been computed, the standard ROM eigenvalues and eigenvectors are computed with a first-order Taylor series expansion. The approximations are

$$\begin{aligned}\widetilde{\lambda}_i &= \lambda_i^0 + \sum_{j=1}^{m}\frac{\partial\lambda_i}{\partial\psi_j}d\psi_j,\\ \widetilde{\phi}_i &= \phi_i^0 + \sum_{j=1}^{m}\frac{\partial\phi_i}{\partial\psi_j}d\psi_j,\end{aligned} \tag{7}$$

where λ_i^0 and ϕ_i^0 are the average eigenvalue and eigenvector results and the tilde symbol annotates an approximation. The increment $d\psi_j$ is the jth z-score value for a given measured airfoil. A first-order approximation was chosen over higher-order methods because of its simplicity and its accurate performance in the demonstration problem. Further work exploring the use of higher-order methods does have merit of should a situation be found where the current approach has unacceptable accuracy.

The forced response ROM is based on modal domain transformation of the equation of motion using the approximate values for (7) while assuming harmonic forcing and motion:

$$\left(-\omega_f^2 + i2\widetilde{\lambda}_i\omega_f\zeta_i + \widetilde{\lambda}_i^2\right)\widetilde{\alpha}_i = \widetilde{\phi}_i^T f, \tag{8}$$

where ω_f is the forcing frequency, ζ_i is the modal damping, $\widetilde{\phi}_i^T f$ is the approximate modal force, and $\widetilde{\alpha}_i$ is the approximate modal coordinates:

$$\widetilde{\alpha}_i = \frac{\widetilde{\phi}_i^T f}{(\widetilde{\lambda}_i^2 - \omega_f^2) + i(2\widetilde{\lambda}_i\omega_f\zeta_i)}, \tag{9}$$

which gives the participation of the ith approximate mode. The approximate displacement vector, $\widetilde{u}$, is computed in the approximate modal domain:

$$\widetilde{u} = \widetilde{\Phi}\widetilde{\alpha}, \tag{10}$$

where the algebra represents modal summation.

While the ROM presented in this section does reduce the costly modal analysis procedures from expensive matrix computations to simple arithmetic, there is an error introduced in the approximation. The next section describes how to improve this model using the developed error-quantification technique.

4. ERROR QUANTIFIED REDUCED-ORDER MODEL

Models in general have an unquantified error between their result and the true value. Accounting for this error and providing an error bound on the result ensure proper model application. This section develops an approach to quantify the error between the eigensensitivity-based approximate models developed in Section 3 and full FEM solutions. This quantification includes analysis for reducible errors related consistently to design parameter variations, that is, bias and random errors that are irreducible without modifying the model form. This error quantification approach is used to reduce error instead of pursuing higher-order approximation methods to avoid the complexity and to develop the error quantifying approach that is applicable to even these more advanced approximations.

The developed error model is an a posterior model that requires comparison of a limited number, k, of full solutions to the standard ROM. These models are referred to as training models that provide the error analysis data. The error is quantified as the discrepancy vector between standard ROM and full model results:

$$\delta_k = f(\mathbf{z}_k) - \widetilde{f}(\mathbf{z}_k), \quad k = 1, 2, \ldots, p, \tag{11}$$

where the functions represent the simulation of a modal response at the kth vector of z-scores defining an airfoil, and the tilde represents the standard ROM approximation. The analysis of the relationship between the vector δ and the components of $\mathbf{z}_k$ determines the existence of a physical relationship between principal component mode magnitude and discrepancy. A discrepancy model as a function of z-scores is constructed from the regression analysis:

$$\delta = \mathbf{F}\beta + \varepsilon, \tag{12}$$

where $\mathbf{F}$ is a matrix of defined regression functions, β is a vector of unknown regression coefficients, and ε is a normally distributed zero mean error term. In the error-quantified ROM, the regression functions are components of the $\mathbf{Z}$ matrix that defines the airfoil geometries. As an example, the matrix form for a regression model that includes a constant and all linear terms is

$$\mathbf{F} = \begin{bmatrix} 1 & \mathbf{Z}_{1,1} & \mathbf{Z}_{1,2} & \cdots & \mathbf{Z}_{1,p} \\ 1 & \mathbf{Z}_{2,1} & \mathbf{Z}_{2,2} & & \\ \vdots & & & \ddots & \\ 1 & & & & \mathbf{Z}_{m,p} \end{bmatrix}, \tag{13}$$

where the first column is the regression coefficient for the constant model term b_0. Should the discrepancy data show nonlinear characteristics, additional nonlinear regression terms can be added. The regression coefficients are determined so that the error between the regression model and the data is minimized through solution of the linear least-squares problem:

$$\left(\mathbf{F}^T\mathbf{F}\right)^{-1}\mathbf{F}^T\delta = \begin{bmatrix} b_0 \\ b_1 \\ \vdots \\ b_m \end{bmatrix}, \tag{14}$$

where b values are the most likely estimates of the regression coefficient vector β. The error term, ε, should be uncorrelated, normally distributed with zero mean and constant variance for statistical modeling assumptions to be met that allow confidence interval prediction. The linear model developed from (12) is added to the approximate model developed in Section 3 to develop the error-quantified ROM for the pth airfoil:

$$\begin{aligned} \widetilde{\lambda}_i &= \lambda_i^0 + \sum_{j=1}^{n} \frac{\partial \lambda_i}{\partial \psi_j} d\psi_j + \left(\mathbf{z}_p^*\right)^T \beta + \varepsilon_p, \\ \widetilde{\phi}_i &= \phi_i^0 + \sum_{j=1}^{n} \frac{\partial \phi_i}{\partial \psi_j} d\psi_j + \left(\mathbf{z}_p^*\right)^T \beta + \varepsilon_p, \end{aligned} \tag{15}$$

where $\mathbf{z}_p^*$ is the vector of z-scores for the pth airfoil with the addition of a leading value of one to account for the constant b_0 term. Because the error terms are modeling error as the difference between full FEM and standard ROM, the addition of these terms reduces the error. Predictor variables, members of β, are only included in the model if they show statistical significance to the error. An advantage of this process is that the PCA produces an orthogonal set of predictor variables which simplifies determination of the parameter significance. These error-quantified modal quantities are then used in an error-quantified forced response solution using the modal domain approach from the previous section.

5. NUMERICAL RESULTS

The sensitivity of blade-alone modal and forced response to geometric deviations from design intent and the effectiveness of both the standard ROM and error-quantified ROM is shown on an advanced sixteen-bladed low-aspect ratio IBR. This IBR, the advanced damping low-aspect ratio fan (ADLARF), has been rigorously studied under the GUIde consortium, a joint government, university, and industrial program to fund research in turbomachinery forced response [15–17]. Because airfoil geometry measurements are not available for this rotor, measured deviations from a related industrial IBR fan stage are used. Full FEMs of the as-measured models of the sixteen airfoils are used to assess sensitivity to variations from design intent, create the error model training data, and quantify the accuracy of the two developed ROMs. While these ROMs do not directly provide mistuning results, they provide the required data for previously referenced mistuning models that account for structural coupling.

Modal calculations were made with a blade-alone finite element fan blade model. The blade approximately spans 12 inches with a 9-inch chord length. The model contains linear hexahedral elements with an element edge length on 0.25 inches, resulting in 7722 degrees-of-freedom, uses common Ti 6Al-4V material properties, and all degrees of freedom are fixed at the blade root. This is a high quality, but not fully converged model, that was used to reduce computational requirements during the development process. A more rigorous converged mesh analysis was

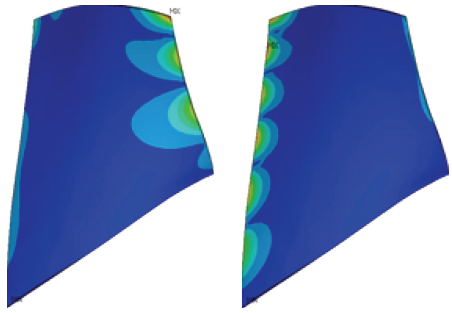

Mode 15 Mode 16

(a) (b)

Figure 1: Mode fifteen and mode sixteen.

conducted to ensure that the unconverged model does not impact any of the research conclusions. The converged model had nearly 50 000 degrees-of-freedom, and frequency variation results for the as-measured models, for the twentieth and most complex mode, were within a maximum of 0.02 percent between the investigated and converged models. This demonstrated that the geometric deviations had nearly the same percentage effect on response variation regardless of mesh density.

Results are obtained from the first twenty modes, covering responses from first flex at 360 Hz to approximately 7000 Hz. Figure 1 shows the mode shapes for the fifteenth and sixteenth modes, which are discussed in greater detail in the proceeding sections. The models were created parametrically with the coordinate measurement machine data points used as the parameters. With this model, airfoil geometry variations were automatically generated through a script file, and mesh topology remained consistent with each model. Post processing was also conducted through scripting to ensure error-free result tabulation.

5.1. Reduced-order geometry model results

An available set of compressor airfoil measured geometry deviations and the ADLARF nominal geometry provided representative as-measured geometry. Figure 2 shows one measured geometry deviation profile representative of the remaining airfoils, both as a blade surface contour plot and a three-dimensional surface plot. Correlation between surface deviation across the blade is evident and shows that a reduced-order geometry model should account for spatial correlation. The measurement also shows negative deviations near the tip and positive deviations near the base. Such a pattern could be developed from variations in the vertical alignment of the part during manufacture. The probability distribution of the set of all measured deviations which is non-Gaussian has a mean value of nearly zero, a standard deviation of 0.003 inches, a minimum of −0.015 inches, and maximum of 0.011 inches.

PCA of the sixteen measured blades generates fifteen principal components, $\Psi \in R^{3n,15}$. Figure 3 shows the percentage total variance of each principal component mode, and it is shown that the first fifteen modes capture all measured deviations. As expected, the modes are ordered by decreasing variance modeling. Because fifteen features fully describe the blade geometry deviations, there is a significant computational cost reduction associated with the Taylor series approximations. If PCA had not reduced the geometry deviation degrees-of-freedom to fifteen, one sensitivity calculation would be needed for each FEM surface node degree-of freedom, requiring nearly 2700 simulations.

5.2. Standard and error-quantified reduced-order model results

The ROMs developed in Sections 2 and 3 are demonstrated on the as-measured rotor. Each subsection first includes results showing the full FEM predicted response variations of the sixteen as-measured airfoils. These results justify the need to account for geometrically induced variations. The subsections then continue to show the ROM's accuracy in predicting blade-to-blade variations for a selected critical mode that provides the training data used to determine the model bias and random error and the two ROM's maximum errors over the first twenty modes.

5.2.1. Frequency results

The IBR frequency variation predicted from the sixteen as-measured airfoils for the first twenty modes, normalized by the average frequency, is shown in the Figure 4 box-and-whisker plot. A box-and-whisker plot displays the four quartiles of data for each data set, displaying the median as the horizontal dash bisecting the rectangular box into the first upper- and lower-data quartiles. The dashed vertical lines attached to these boxes show the upper- and lower-second quartiles. Addition symbols are for outlier data. Results show the largest frequency variation interval covering greater than ±2% of the average value for sixteenth mode with the mean range of variation for all modes nearly ±1%. It is seen that the normalized frequency deviation does not appear to significantly increase with the increasing mode number because of the normalization. The absolute variation in frequency does increase with mode number. Further analysis of the coefficient of variation, the data mean divided by its standard deviation, does show an increasing trend in normalized variation.

While these are small deviations, they are in a range shown to lead to maximum mistuning amplifications. The close proximity of blade-to-blade frequencies causes multiple mode excitations at a single forcing frequency and summation of modal energy. Mistuning response will be highly sensitive to the exact pattern, so accurate prediction of each blade frequency is required. The predicted frequency variations can provide the necessary input to existing mistuned forced response ROMs and avoids experimental frequency measurement. Explicit geometric modeling also physically links design parameters to the frequency variations that lead to mistuned amplification. Understanding gained through these ROMs can lead to design changes or manufacturing process controls that will lead to improved IBR reliability.

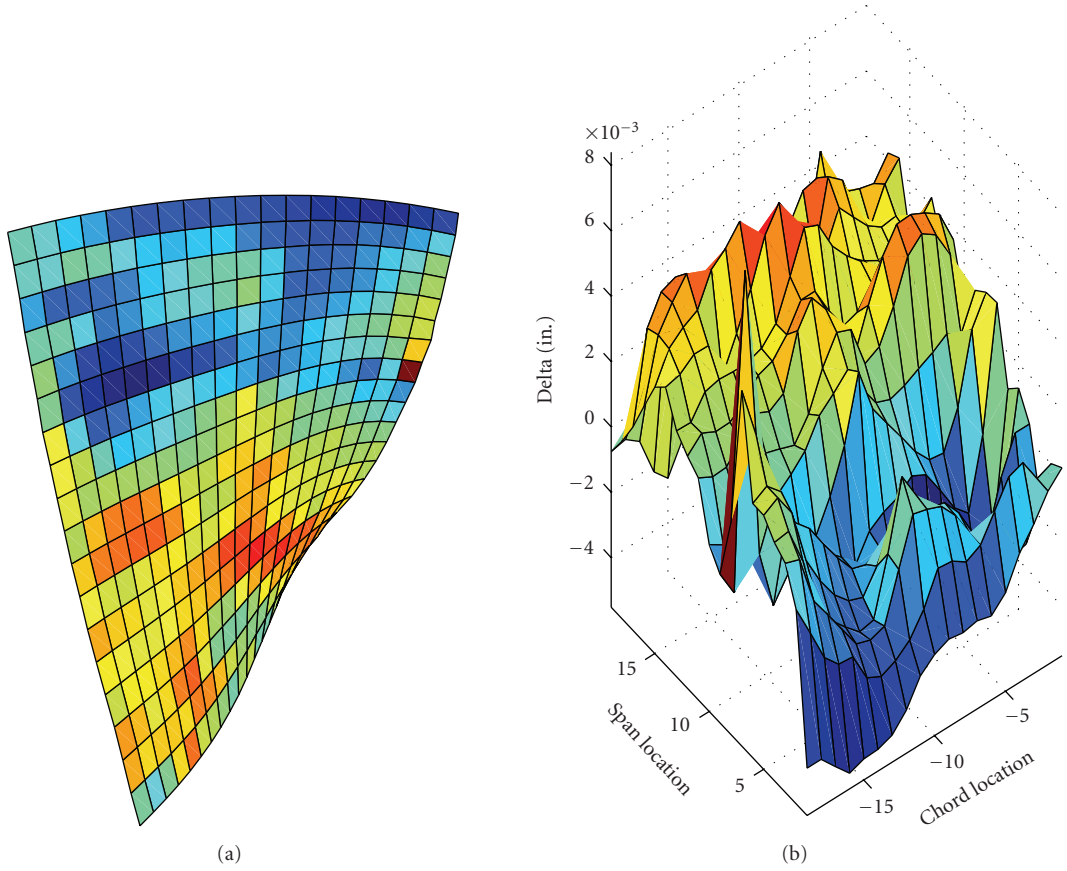

Figure 2: Airfoil surface deviation (Blade 1).

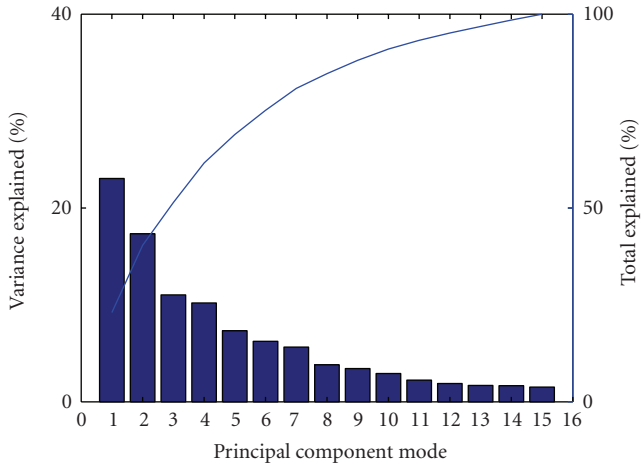

Figure 3: Total variance explained by principal components.

Figure 5 plots the comparison between the predicted blade-to-blade IBR frequencies from the full finite element model, standard ROM, and the error-quantified ROM. Results for the sixteenth mode are shown because it had the largest frequency scatter in the first twenty modes, as seen in Figure 4, and also have the largest error between full model and standard ROM predictions as shown in Figure 7. Even though Figure 5 shows the ROMs at their worst, it is seen that the standard ROM does an admirable job predicting blade-to-blade frequency deviations and captures the blade-to-blade trend in frequency deviation. Because mistuning is highly sensitive to frequency magnitudes, a reduced error model is still desirable. Results show that the error-quantified ROM greatly improved accuracy. The airfoils with the greatest error from the standard ROM, three, four, eight, ten, fifteen, and sixteen show a marked improvement with the error-quantified ROM.

The input for the bias and random error terms of the error-quantified ROM was constructed from the a posterior discrepancy analysis between full FEM and standard ROM. Figure 6 shows the errors for the sixteenth mode plotted against the z-scores of the retained principal component modes. There is a clear linear correlation between the residual value and the z-score magnitude of the twelfth principal component mode, while all other modes appear randomly distributed. This linear relationship was seen for all twenty modes. Because there is a predictable trend between the residual and twelfth principal component mode magnitude, the error quantified reduced-order model from (15) will account for model bias and improve accuracy. Each mode has its own regression coefficients based on that mode's data. The remaining error not accounted for as bias

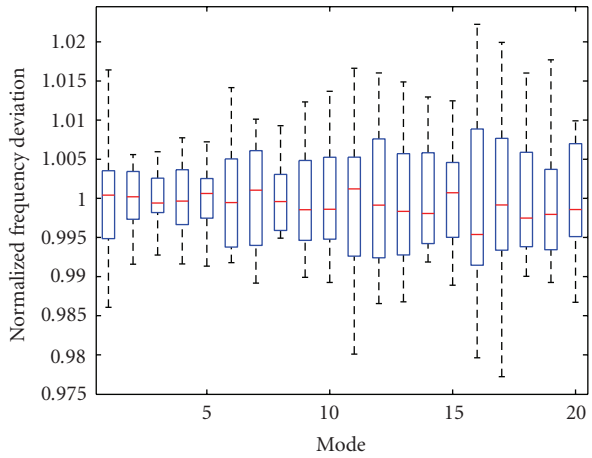

Figure 4: Airfoil frequency variation.

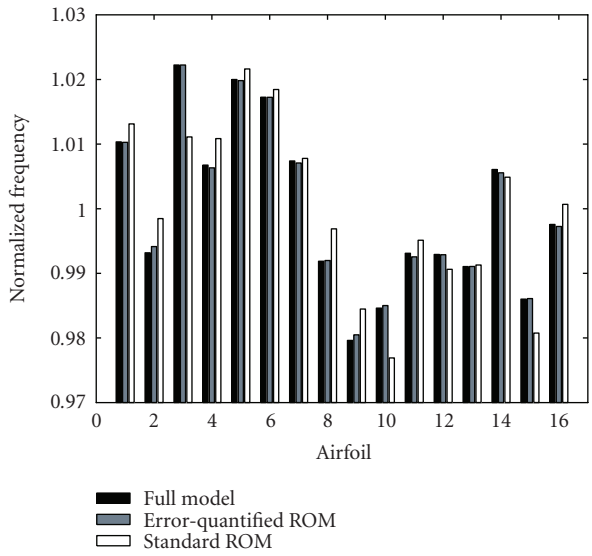

Figure 5: Frequency prediction comparison (Mode 16).

can be included in the random error parameter of the error-quantified ROM.

It is noted that standard regression modeling practice avoids validating the model with the data used to create the regression model. This practice was not followed for the results shown. This is acceptable because the strong linear relationship in the data shows that the result is more than just a random phenomenon. Nonetheless, a set of 50 randomly generated airfoil geometries based on the statistics from the PCA analysis was analyzed with the full FEM and ROMs. These results did not change any of the conclusions based on the sixteen as-measured airfoils and show that the error-quantified model is applicable to the larger domain of random airfoils.

Figure 7 shows the maximum percent error between the two ROMs and the full FEM for all twenty vibration modes. This maximum error is obtained for each mode by computing the absolute difference between each ROM and full model, dividing by the full model value for each of the sixteen airfoils and plotting only the maximum of these sixteen error results. This is again a worst case looks at the models, and the average blade error of the ROMs is significantly lower as can be seen in Figure 5. Figure 7 shows that while the standard ROM had a maximum percent error below 0.5% for the first 10 modes and below 1% for all but one of the remaining modes, the error-quantified ROM predicted much improved results nearly identical to the full model. Error percentages from the error-quantified ROM for the first twenty modes are below 0.1% error. The figure shows that the error-quantified ROM reduced the maximum percent error for all the first twenty modes by well over 75%. While the standard ROMs accuracy may be considered sufficient, the high sensitivity of mistuned response to variations on the order of its error indicates that the error-quantified model may be more appropriate.

5.2.2. Modal force results

While frequency deviation has been a subject of study because of its relevance to frequency-based mistuning ROMs, mode shape deviation has received limited investigation. In this section, the mode shape variations are not shown directly, instead the useful heuristic of modal force deviations is shown because of its role in forced response prediction. Modal force, the inner product of the mode shape and loading vectors, is the quantity on the right-hand side of the modal equation of motion, and its variation has a $1:1$ correspondence to forced displacement variation. Nominal unsteady loading predictions for a defined harmonic from a related IBR were used in the modal force calculation.

A modal force variation box-and-whisker plot for the as-measured IBR is shown in Figure 8. It is evident that these deviations are much larger than the frequency scatter. The first significant variation in modal force is shown at the fifth mode with an upper bound 29% larger than the average value. Considering the set of the first twenty modes, several modes are observed with upper bounds near 20%, with mode fifteen notable for a 55% upper bound. These significant variations in modal force directly impact variation in airfoil forced response, and these are not explicitly accounted for in current design or mistuning analysis practices. These variations are in addition to those blade-to-blade stress variations caused by mistuning, that should be accounted for to reliably predict forced response variations, and demonstrate the need for a eigenvector response ROM that accounts for geometry variation.

Figure 9 plots the blade-to-blade comparison between the full FEM, the standard, and error-quantified ROMs for the fifteenth mode modal force prediction. The fifteenth mode was selected because the as-measured airfoil results for this mode had the largest modal force variation, shown in Figure 8, and also has the largest error between standard ROM and full models as seen in Figure 11. Again, this shows the two ROMs at their worst. As seen in Figure 9, the standard ROM accurately captures the trend of modal force variation. The error-quantified ROM improves the approximation for nearly all airfoils, in particular the third,

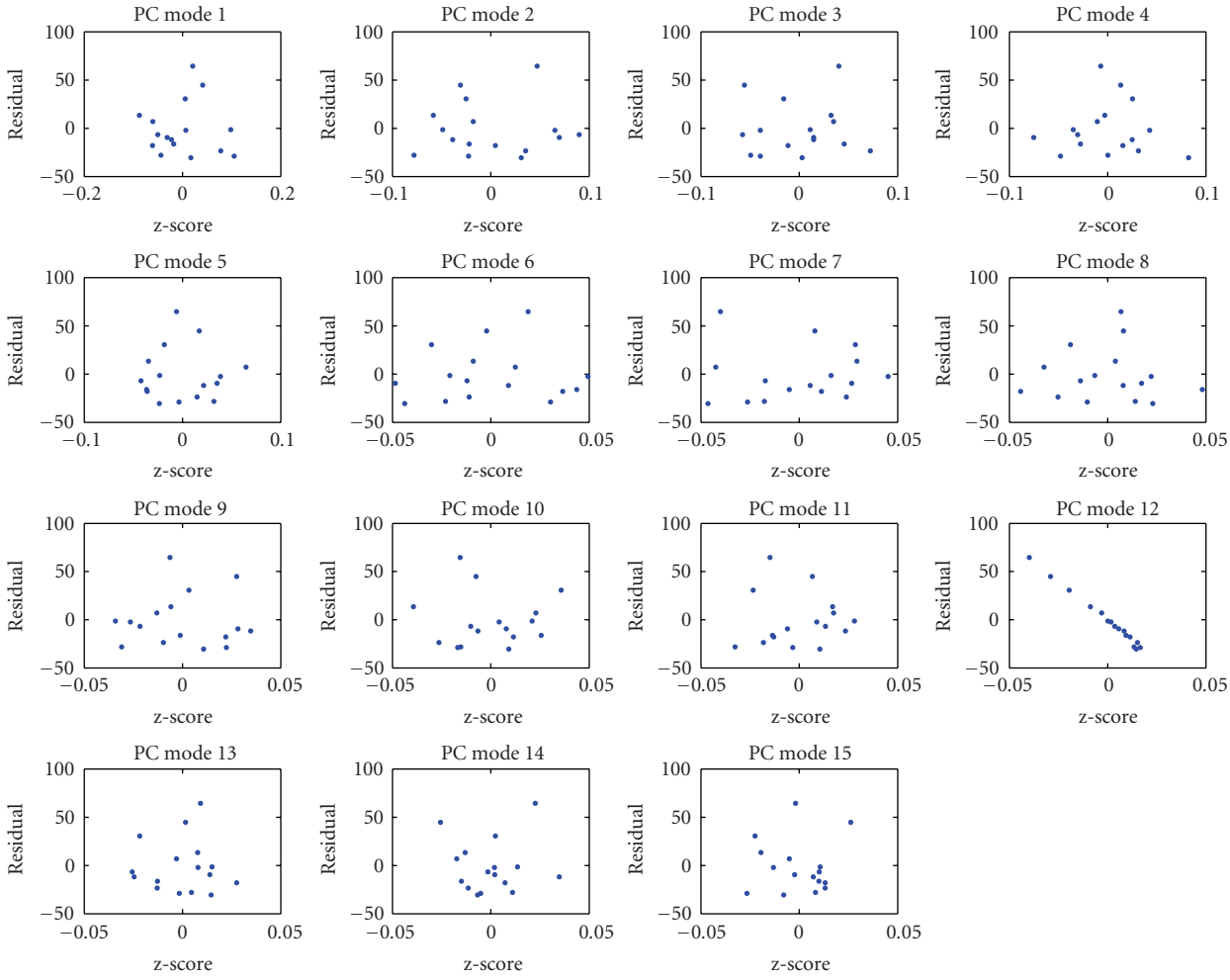

Figure 6: Correlation of PC mode parameters and frequency residual (Mode 16).

fourth, eighth, tenth, fifteenth, and sixteenth airfoil. These airfoils are the same that were shown to have the largest frequency error, also had the largest modal force error, and were also effectively accounted for by the error-quantified ROM.

The discrepancy calculated between the standard ROM and full FEM modal force solutions of the as-measured IBR is plotted with respect to the airfoil z-scores in Figure 10. Again as with the frequency results, principal component mode twelve shows a linear relationship between the error and airfoil z-score value. When compared to the frequency residuals of Figure 6, the linear relationship is still obvious but with more random variation.

Figure 11 plots the maximum error between the full FEM and ROMs for the first twenty modes. This maximum error is obtained for each mode by computing the absolute difference between standard ROM and full model, dividing by the full model value for each of the sixteen airfoils and plotting only the maximum of the sixteen errors. It is initially observed that the errors are significantly larger than for frequency, but this is not unexpected as the variations in modal force are significantly larger. For the first twenty modes, the standard ROM performs adequately with more than half the modes below 5% and most remaining modes below errors below 10% with the exception of the thirteenth, fifteenth, and nineteenth modes. The error-quantified ROM reduces the error for these modes in addition to significant error reduction for the fifth mode. The error-quantified ROM reduces the error for these modes by over 50%. In general, it is seen that the error-quantified model is providing a reduced benefit to the ROM when compared to the frequency results, but still enables more accurate modal force prediction for the first twenty modes within 6% of full model results. The remaining error can be accounted for with the error-quantified ROM random error term.

5.2.3. *Forced response results*

While the variation in modal force is a significant contributor to forced response, it only accounts for variations in mode shape displacements. Variations in modal stress and frequency will also impact forced response variation and

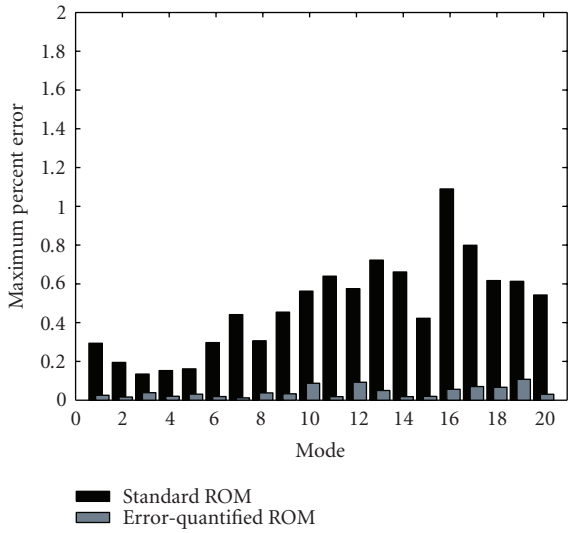

Figure 7: Maximum error calculation for airfoil frequency.

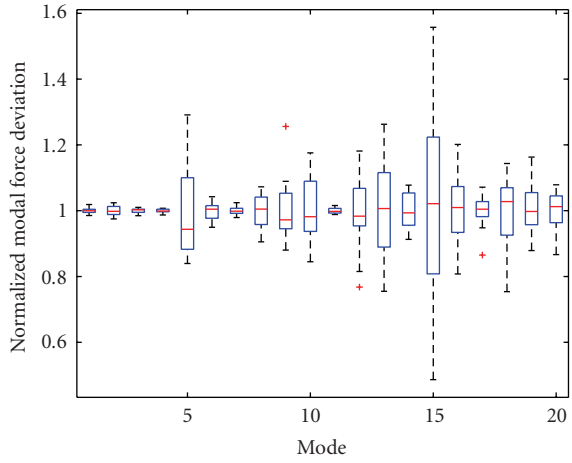

Figure 8: Airfoil modal force variation.

this section's results account for those effects. The maximum forced stress variation box-and-whisker plot is shown in Figure 12. Considering the set of the first twenty modes, several modes are observed with upper bounds near 20%, with mode fifteen notable for a 68% upper bound.

Comparison of these plots to the modal force variation results of Figure 8 shows similar magnitudes of variation for each mode, but closer inspection shows differences on many modes. Mode nine's upper bound on airfoil forced response is 38% greater than average airfoil, while its modal force upper bound was 19%. Mode fifteen shows a 68% increase in upper bound stress while the modal force upper bound variation for the mode was 55%. These 19% and 13% increases in stress upper bounds are caused by variations in the maximum modal stress caused by geometric deviations. This demonstrates the importance of accounting for modal stress variations in the developed ROMs.

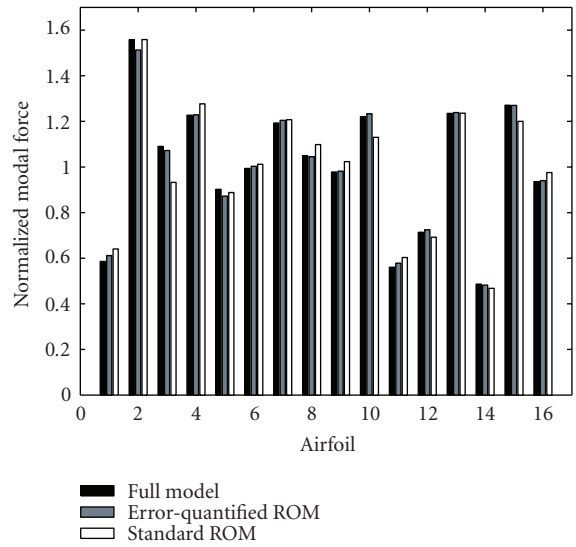

Figure 9: Modal force prediction comparison (Mode 15).

The maximum forced stress blade-to-blade prediction is compared between the standard ROM, error-quantified reduced-order ROM, and full model in Figure 13. The fifteenth mode was selected because the as-measured results for this mode, shown in Figure 8, had the largest forced response scatter and also has the largest error between full models and standard ROM, shown in Figure 14. Figure 13 shows that the standard ROM does a good job representing the full model results and accurately captures the blade-to-blade trend in forced stress values. The figure also shows that the error-quantified ROM improves the approximation for all airfoils, in particular the third, fourth, eighth, tenth, fifteenth, and sixteenth airfoil.

The a posterior training data used to create the error quantified reduced-order model is not shown but is almost identical to Figure 10.

Figure 14 plots the maximum error between the ROMs and the full models for the first twenty modes. For these modes, the standard ROM does well with most errors below 5%, with the exception of modes five, fifteen, and sixteen. The error-quantified ROM reduces the error for many of the larger errors in this range, particularly modes five, fifteen, and sixteen where error is reduced by nearly 50%. In general, it is seen that the error-quantified model is not as effective in correcting for bias as it was for frequency but still enables forced response force prediction for the first twenty modes within 5% of full model results. The remaining random error can be accounted for with the random error term.

5.3. Explanation of error root cause

It is necessary to consider why a single principal component mode has shown such a strong linear relationship to error. While a precise explanation is not possible, there are several factors which lead to a supported argument. First, the linear approximations of frequency by the standard first-order sensitivity ROM work well, and further analysis demonstrated

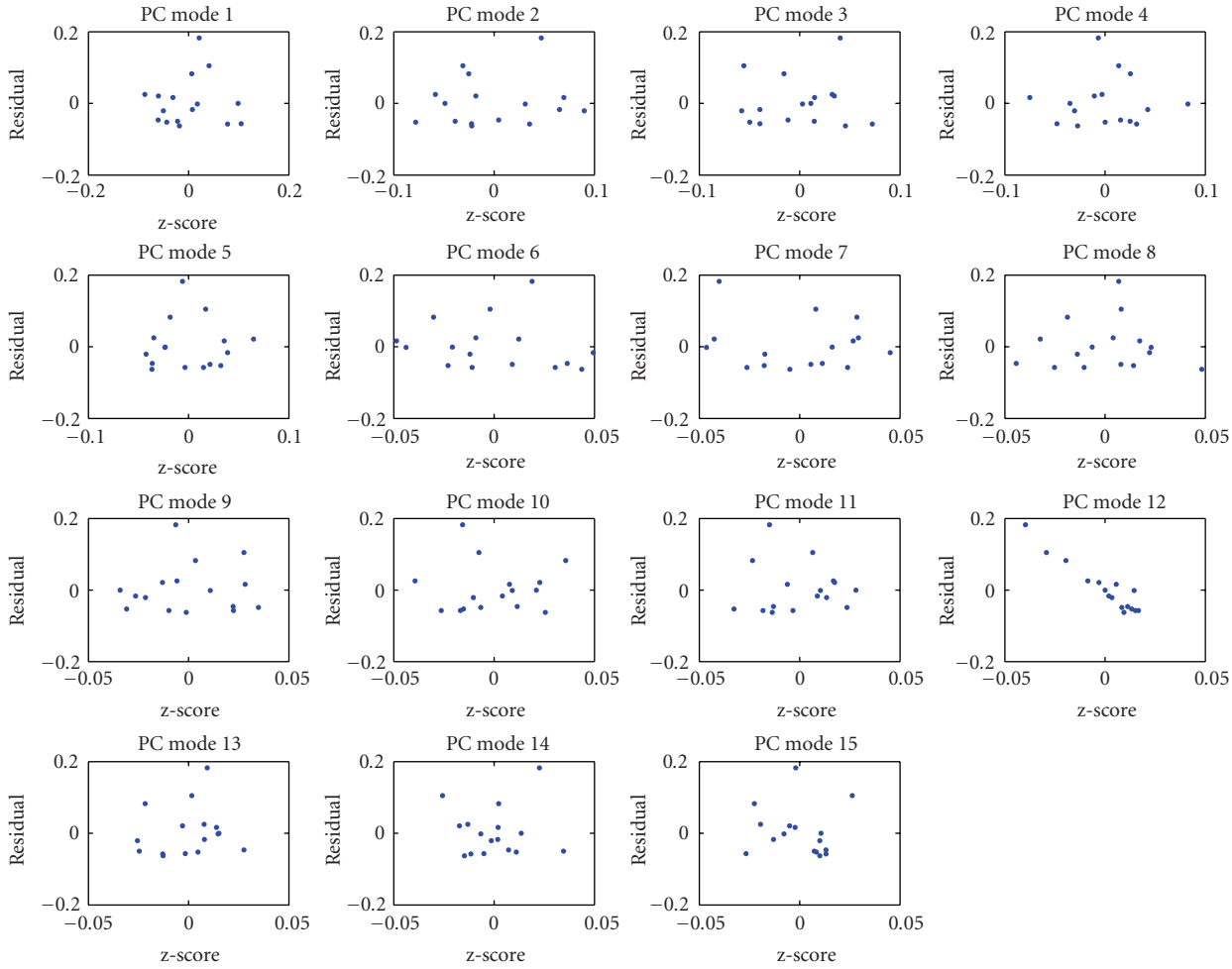

Figure 10: Correlation of PC mode parameters and modal force residual (Mode 15).

that the frequency deviations over the range considered and for a single PCA mode are practically linear. It is then also significant that the relationship between frequency error and the twelfth PCA mode participation is likewise practically linear. Therefore, there is a clear evidence that the sensitivity of the twelfth PCA mode has been inaccurately calculated because the magnitude of the PCA mode is still enabling an improved prediction. Because an automated process was used to generate input files and process results, it is not likely that a user-based processing error was the cause of this error. It is then likely that the error resides in the numerical accuracy of the finite element solution software used in this effort. The magnitude of the twelfth mode was smaller relative to the other modes, and it is possible it fell below a limit that the software was able to accurately consider independently from the other variations. While this error could be addressed with FE software improvements, the error-quantified model shows its benefit by both identifying the error, what parameter is causing it, and also correcting the model. The model also retains its value of accounting for random errors, which is significant when conducting a probabilistic analysis or developing predictive confidence bounds.

6. CONCLUSION

This effort demonstrated the impact of geometry deviations from design intent on the modal and forced response behavior of airfoils. Significant variations were shown on frequency and these variations are significant to mistuned rotor response. The ability to predict these efficiently with the developed ROMs can significantly improve current mistuning analysis and design procedures. It was shown that mode shape variations were more sensitive than frequency variations and these led to large variations in forced response. These variations are not currently accounted for in design, but the developed ROMs begin the process to do so. The ROMs are based on PCA reduction in geometry parameters and an eigensensitivity-based approximation to reduced response solution times. The error between this model and full models was quantified, and a linear regression model was demonstrated to quantify which parameter was

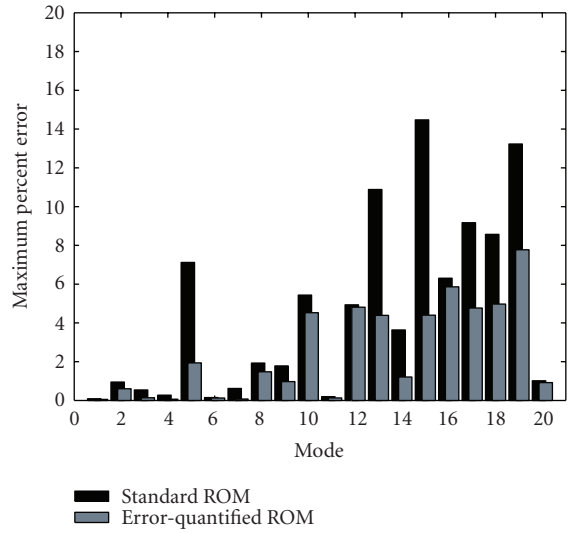

Figure 11: Maximum error calculation for airfoil modal force.

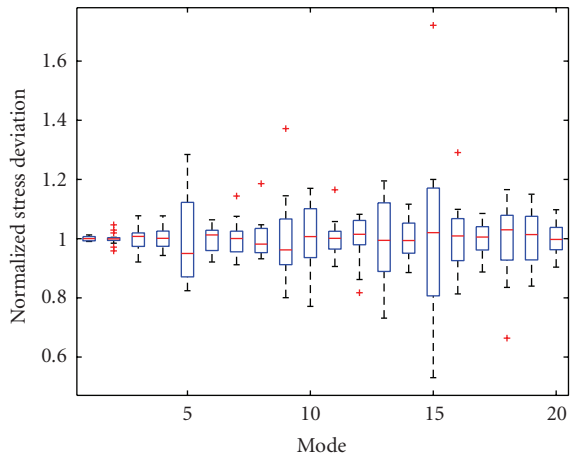

Figure 12: Airfoil forced stress variation.

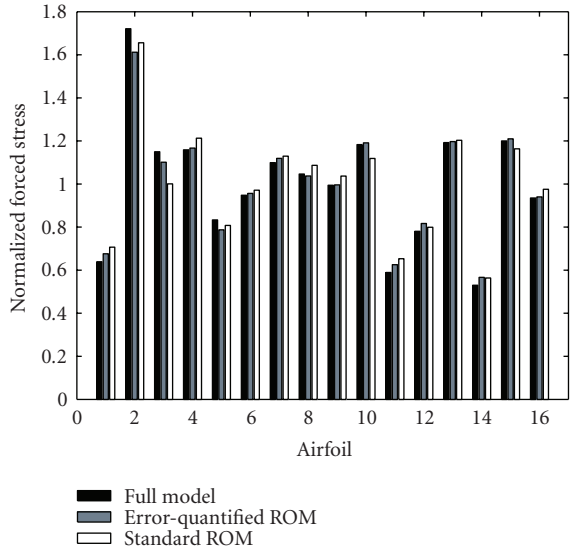

Figure 13: Forced stress prediction comparison (Mode 15).

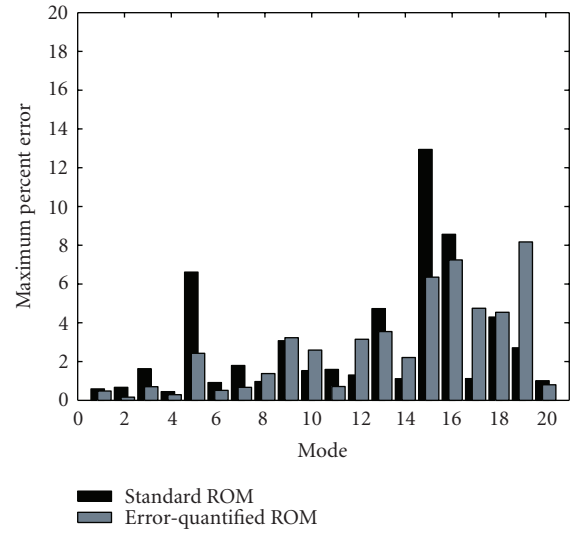

Figure 14: Maximum error calculation for airfoil forced stress.

contributing to error. Knowledge of this relationship led to an improvement in the model accuracy. The error was likely caused by limitations in the numerical accuracies of the FE software and this was corrected by the error-quantified ROM.

REFERENCES

[1] R. Bladh, M. P. Castanier, and C. Pierre, "Component mode based reduced order modeling techniques for mistuned bladed disks part 1: theoretical model," *Journal of Vibration and Acoustics*, vol. 123, no. 1, pp. 89–99, 2001.

[2] M. P. Castanier, G. Ottarsson, and C. Pierre, "A reduced-order modleing technique for mistuned bladed disks," *Journal of Vibration and Acoustics*, vol. 119, no. 3, pp. 439–447, 1997.

[3] D. M. Feiner and J. H. Griffin, "A fundamental model of mistuning for a single family of modes," *Journal of Engineering for Gas Turbines and Power*, vol. 124, no. 4, pp. 597–605, 2002.

[4] J. H. Griffin, "On predicting the resonant response of bladed disk assemblies," *Journal of Engineering for Gas Turbines and Power*, vol. 110, pp. 45–50, 1988.

[5] E. P. Petrov, K. Y. Sanliturk, and D. J. Ewins, "A new method for dynamic analysis of mistuned bladed disks based on the exact relationship between tuned and mistuned systems," *Journal of Engineering for Gas Turbines and Power*, vol. 124, no. 3, pp. 586–597, 2002.

[6] M. T. Yang and J. H. Griffin, "A reduced-order approach for the vibration of mistuned bladed disk assemblies," *Journal of Engineering for Gas Turbines and Power*, vol. 119, no. 1, pp. 161–167, 1997.

[7] V. E. Garzon and D. L. Darmofal, "Impact of geometric variability on axial compressor performance," *Journal of Turbomachinery*, vol. 125, no. 4, pp. 692–703, 2003.

[8] I. T. Jolliffe, *Principal Component Analysis*, Springer, New York, NY, USA, 1986.

[9] E. Capiez-Lernout, C. Soize, J.-P. Lombard, C. Dupont, and E. Seinturier, "Blade manufacturing tolerances definition for a mistuned industrial bladed disk," *Journal of Engineering for Gas Turbines and Power*, vol. 127, no. 3, pp. 621–628, 2005.

[10] R. L. Fox and M. P. Kapoor, "Rates of change of eigenvalues and eigenvectors," *AIAA Journal*, vol. 6, no. 12, pp. 2426–2429, 1968.

[11] M. I. Friswell, "The derivatives of repeated eigenvalues and their associated eigenvectors," *Journal of Vibration and Acoustics*, vol. 118, no. 3, pp. 390–397, 1996.

[12] P. J. Roache, K. Ghia, and F. White, "Editorial policy statement on the control of numerica accuracy," *ASME Journal of Fluids Engineering*, vol. 108, no. 1, p. 2, 1986.

[13] AIAA, "Editorial policy statement on numerical accuracy and experimental uncertainty," *AIAA Journal*, vol. 32, no. 1, p. 3, 1994.

[14] R. T. Haftka and Z. Gurdal, *Elements of Structural Optimization*, Kluwer Academic Publishers, Norwell, Mass, USA, 3rd edition, 1992.

[15] S. E. Gorrell and M. W. Davis, "Application of a dynamic compression system model to a low aspect ratio fan: casing treatment and distortion," in *Proceedings of the 29th AIAA/ASME/ASCE/AHS/ASC Structures, Structural Dyanmics, and Materials Conference*, AIAA, Monterey, Calif, USA, June 1993, AIAA paper 93-1871.

[16] C. Bréard, M. Vahdati, A. I. Sayma, and M. Imregun, "An integrated time-domain aeroelasticity model for the prediction of fan forced response due to inlet distortion," *Journal of Engineering for Gas Turbines and Power*, vol. 124, no. 1, pp. 196–208, 2002.

[17] S. R. Manwaring, D. C. Rabe, C. B. Lorence, and A. R. Wadia, "Inlet distortion generated forced response of a low aspect ratio transonic fan," in *Proceedings of the International Gas Turbine and Aeroengine Congress and Exposition (Paper)*, p. 14, Burmingham, UK, June 1996, ASME paper 96-GT-376.